

## Absence of Debye Sheaths due to Secondary Electron Emission

M. D. Campanell, A. V. Khrabrov, and I. D. Kaganovich

*Princeton Plasma Physics Laboratory, Princeton University, Princeton, New Jersey 08543, USA*

(Received 19 January 2012; published 18 June 2012)

A bounded plasma where the hot electrons impacting the walls produce more than one secondary on average is studied via particle-in-cell simulation. It is found that no classical Debye sheath or space-charge-limited sheath exists. Ions are not drawn to the walls and electrons are not repelled. Hence the unconfined plasma electrons travel unobstructed to the walls, causing extreme particle and energy fluxes. Each wall has a *positive* charge, forming a small potential barrier or “inverse sheath” that pulls some secondaries back to the wall to maintain the zero current condition.

DOI: [10.1103/PhysRevLett.108.255001](https://doi.org/10.1103/PhysRevLett.108.255001)

PACS numbers: 52.40.Kh, 52.40.Hf, 52.65.Rr

Any unbiased material in contact with a plasma must draw zero current in equilibrium. Generally, the thermal velocity of electrons far exceeds that of ions. So the material charges negatively. A Debye sheath [1] forms at the boundary. There are many versions [2,3] of sheath theory for various applications, but the qualitative features are similar. The sheath accelerates ions to the surface and forms a potential barrier to incoming electrons of magnitude  $\Phi$  needed to maintain equal fluxes,  $\Gamma_e = \Gamma_i$ . Sheath theory is essential for studying plasma-wall interaction, setting boundary conditions in fluid simulation codes [2,4] and measuring plasma properties with Langmuir probes [3].

Bombardment from plasma electrons may eject electrons from a material. For most materials in the energy range of interest,  $\gamma(\varepsilon)$ , the average number of “secondaries” produced by an incident electron, increases with impact energy  $\varepsilon$  [5]. Secondary electron emission (SEE) alters the current balance. Let  $\gamma_{\text{net}} \equiv \Gamma_{\text{out}}/\Gamma_{\text{in}}$  denote the ratio of emitted flux to incident electron flux at a wall. The zero current condition becomes

$$\Gamma_e = \Gamma_{\text{in}} - \Gamma_{\text{out}} = \Gamma_{\text{in}}(1 - \gamma_{\text{net}}) = \Gamma_i. \quad (1)$$

$\gamma_{\text{net}}$  depends on the distribution of impact energies and generally increases with temperature  $T_e$ . As  $\gamma_{\text{net}}$  increases,  $\Phi$  decreases because more electrons must reach the wall to balance the ion flux (which is independent of  $\Phi$  by the Bohm criterion [1,6]). At higher temperatures as  $\gamma_{\text{net}} \rightarrow 1$ , the influx increases rapidly because  $\Gamma_{\text{in}} = \Gamma_i/(1 - \gamma_{\text{net}})$ . Before  $\gamma_{\text{net}}$  reaches unity, the emission  $\Gamma_{\text{out}} = \gamma_{\text{net}}\Gamma_i/(1 - \gamma_{\text{net}})$  becomes intense enough that the negative charge formed by secondaries at the interface creates a potential barrier that reflects some cold secondaries back to the wall [7]. In principle, this allows zero current to be maintained even if the emission induced by hot plasma electrons exceeds unity. The *net* emission  $\gamma_{\text{net}}$  saturates to a critical value  $\gamma_{\text{cr}} < 1$  so that  $\Gamma_i$  in (1) can still be balanced. The “space-charge-limited” (SCL) sheath is usually assumed to form under very strong emission in tokamaks [4,8], Hall

thrusters (HTs) [9], emissive probes [2,10], and general plasma-wall systems [3,7,11].

Theories invoking the SCL sheath rely on a sheath structure existing *a priori* as the SEE intensity increases beyond the threshold for saturation. For instance, the original Hobbs-Wesson paper [7] assumes ions “arrive at the sheath edge” with a velocity related to the Bohm criterion. Poisson’s equation is then solved with charge densities in the sheath written in terms of a potential *assumed* below the plasma potential. However, suppose a material is suddenly inserted into a hot plasma. The initial rush of electrons with  $\gamma(\varepsilon) > 1$  will cause *reduction* of electrons on the surface and ions would then be repelled from the surface. The assumptions [1,3,6] inherent in deriving the Bohm criterion are not satisfied, e.g., that the wall potential is below the plasma potential and that ions are drawn to the wall. Morozov and Savel’ev [12] have shown that for a plasma-wall-SEE system with a Maxwellian electron velocity distribution function (EVDF) at infinity, at high temperatures there are potential profile solutions in which the wall potential is indeed above the plasma potential. Overall, it is unclear whether a sheath could form in the first place if SEE is very strong.

In this Letter, we study directly by simulation a plasma in which the hot electrons impacting the walls on average have  $\langle \gamma(\varepsilon) \rangle > 1$ . This situation may naturally arise, for example, in a Hall discharge when the drift velocity  $V_D$  is large. We simulate such a plasma using EDIPIC (electrostatic direct implicit particle-in-cell) code and show the behavior is unexplained by familiar theories. In particular, there is no classical sheath or SCL sheath. Electrons travel unimpeded to the walls. The plasma in this new regime is dramatically different than in past EDIPIC simulations [13–17] with smaller drift energy.

EDIPIC code simulates a planar  $\mathbf{E} \times \mathbf{B}$  xenon plasma bounded by floating walls made of boron-nitride ceramics (BNC); see Fig. 1(a). Details on the numerical algorithms, verification, and past results are provided in Ref. [17]. Both the plasma and sheath regions are resolved. The applied fields  $E_z$  and  $B_x$  are uniform. Ions and electrons are treated

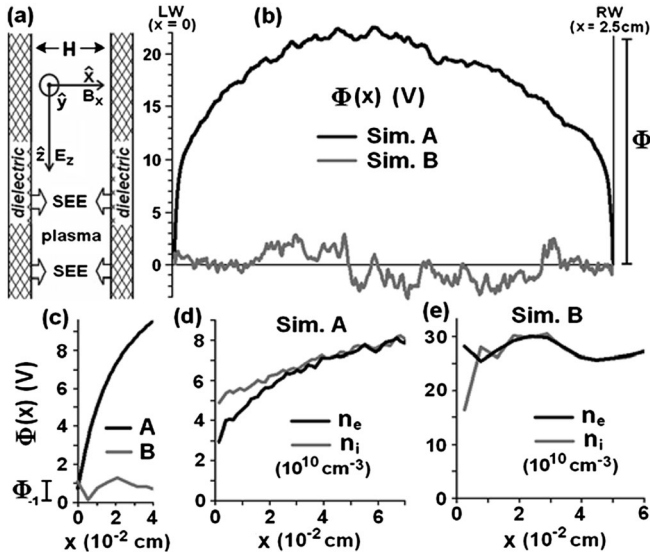


FIG. 1. (a) Simulation model. (b)  $\Phi(x)$ . (c)  $\Phi(x)$  near the left wall (LW). Electron and ion densities near the LW in simulation A (d) and simulation B (e). Snapshots (b)–(e) represent  $t = 10 \mu\text{s}$  in both runs.

as particles. The plasma is given an initial density  $n_0$  and allowed to evolve. Particle dynamics are governed by the plasma’s self-generated field  $E_x(x)$  and the  $\mathbf{E} \times \mathbf{B}$  drift motion from the background fields. For electrons, the neutral gas density  $n_a$  determines the frequency of elastic collisions  $\nu_{en}$ . Coulomb collisions are implemented with a Langevin model, but can usually be neglected as they only weakly affect the plasma [18]. Turbulent collisions of frequency  $\nu_{\text{turb}}$  effectively simulate anomalous conductivity by scattering the  $y$ - $z$  component of the velocity vector [19]. Each scatter leads to displacement along  $E_z$  and an energy gain parallel to the walls on average of  $\langle \Delta W_{\parallel} \rangle = m_e V_D^2$ .

Past simulations modeling the Princeton Plasma Physics Laboratory HT found that, in the low collisionality regime anticipated in experiments, the bulk plasma EVDF is anisotropic and strongly depleted in the loss cone [15]. In contrast to collisional regimes where the SEE thermalizes in the plasma [9], the emitted electrons form beams that cross the plasma and strike the other wall. The particle flux at each wall consists of collision-ejected electrons (CEEs) scattered into the loss cone by impacts with neutrals, “beam” electrons from the other wall, and ions.  $\Gamma_i$  is given by the Bohm criterion in terms of the electron temperature normal to the walls,  $T_x$  [15];  $\Gamma_i \approx (n/2)(T_x/m_i)^{1/2}$ . In quasisteady state, the zero current condition applies. By symmetry, the two beams are equal and opposite. So at each wall, the incident beam and outgoing SEE are equal. Equation (1) becomes  $\Gamma_e = (\Gamma_{\text{CE}} + \Gamma_b) - \Gamma_b = \Gamma_{\text{CE}} = \Gamma_i$ . Also, the SEE produced by  $\Gamma_{\text{in}}$  must yield the outgoing beam  $\Gamma_b$ . That is,  $\gamma_{\text{CE}}\Gamma_{\text{CE}} + \gamma_b\Gamma_b = \Gamma_b$ . We obtain

$$\Gamma_{\text{CE}} \approx \Gamma_i, \quad (2)$$

$$\Gamma_b \approx \frac{\gamma_{\text{CE}}\Gamma_{\text{CE}}}{(1 - \gamma_b)}, \quad (3)$$

$$\gamma_{\text{net}} \approx \frac{\gamma_{\text{CE}}}{(1 + \gamma_{\text{CE}} - \gamma_b)}, \quad (4)$$

where  $\gamma_b$  and  $\gamma_{\text{CE}}$  are the partial SEE coefficients. (e.g.,  $\gamma_{\text{CE}} \equiv$  ratio of secondary flux produced by CEEs to  $\Gamma_{\text{CE}}$ ). It has been found [15] that a classical non-SCL sheath forms even if  $\gamma_{\text{CE}}$  is well above unity because as long as  $\gamma_b < 1$ ,  $\gamma_{\text{net}} < 1$  also via (4). Past simulations typically used  $B_x = 100$  G and  $E_z = 50$ – $200$  V/cm. For  $E_z = 200$  V/cm, it was found that  $\gamma_b$  approaches unity ( $\sim 0.92$ – $0.95$ ). This is because the drift energy gained by cold emitted secondaries crossing the plasma can range up to  $2m_e V_D^2 = 45$  eV, so the beam energy can approach the  $\gamma(\varepsilon) = 1$  threshold for BNC, where  $\gamma(\varepsilon) \approx 0.17\varepsilon^{1/2}$  ( $\varepsilon$  in eV) [20].

If  $E_z$  is increased further, the physics fundamentally changes. Simulation A with  $E_z = 200$  V/cm,  $B_x = 100$  G,  $n_a = 10^{12}$  cm $^{-3}$ ,  $n_0 = 10^{11}$  cm $^{-3}$ ,  $\nu_{\text{turb}} = 1.4 \times 10^6$  s $^{-1}$ , and  $H = 2.5$  cm features the familiar behavior discussed previously. We compare it to simulation B with all conditions equal except  $E_z = 250$  V/cm and  $\nu_{\text{turb}} = 2.8 \times 10^6$  s $^{-1}$ . One may expect the plasma in simulation B to be hotter with a larger sheath potential, but otherwise similar to simulation A. Figure 1(b) shows the electrostatic potential function  $\Phi(x)$  in both runs, relative to the right wall. Simulation A exhibits a nearly symmetric potential well of amplitude  $\Phi \approx 21$  V with well-defined sheaths near the walls and presheaths in the interior. (The asymmetry is from fluctuations due to two-stream instability that arise when the SEE beams are intense [21]). However,  $\Phi(x)$  in simulation B has no sheath structure. Two-stream fluctuations of a few volts dominate.

The unusual behavior in simulation B is due to the SEE. The flux components and partial SEE coefficients are listed in Table I. In simulation A, a classical sheath appears because  $\gamma_b < 1$  and thus  $\gamma_{\text{net}} < 1$ . Equations (2)–(4) apply. In simulation B, the  $\mathbf{E} \times \mathbf{B}$  drift energy is  $\sim 50\%$  larger and  $\gamma_b$  actually exceeds unity. Equation (4) suggests a classical sheath cannot exist because  $\gamma_{\text{net}}$  too would exceed unity and  $\Gamma_i$  in (1) could not be balanced. Also, with  $\gamma_b > 1$ , the SEE beams would multiply at each flight between the walls and grow perpetually.

Closer study of the new regime reveals each wall acquires a slight positive charge, as is reasonable to expect if most incident electrons have  $\gamma(\varepsilon) > 1$ . Ions are repelled away from the wall and the net space charge near the interface is negative; see Fig. 1(e). Therefore, at all times it is found that  $\Phi(x)$  decreases from the wall outward; see Fig. 1(c). (These features are all opposite to simulation A.) The small potential barrier at the interface pulls some of the SEE back to the wall. Thus, this “inverse sheath” prevents unbounded charge flow between the plasma and wall, as does a classical sheath. But in contrast, the latter

TABLE I. Key parameters at  $t = 10 \mu\text{s}$  in both runs, after quasisteady state was reached. Fluxes are at the left wall in units of  $10^7 \text{ cm}^2 \text{ ns}^{-1}$ .

Simulation	A	B	A	B
$\gamma_b$	0.94	1.22	$\Gamma_b$	78.7
$\gamma_{\text{CE}}$	1.75	1.28	$\Gamma_{\text{CE}}$	3.21
$\gamma_{\text{net}}$	0.96	1	$\Gamma_o$	N/A
$\langle W_x \rangle$ (eV)	5	2.5	$\Gamma_{\text{in}}$	81.9
$\langle W_{\parallel} \rangle$ (eV)	89	46	$\Gamma_i$	2.51
$\langle V_z \rangle$ (km/s)	-6.5	-50		

works by reflecting a large portion of *hot* plasma electrons *approaching* the wall, requiring a much larger positive amplitude  $e\Phi \sim T_e$ , as in simulation A. Note that while the inverse sheath amplitude  $\Phi_{-1} \approx 1 \text{ V}$  in Fig. 1(c) appears trivial relative to the large fluctuations throughout the plasma domain, only the structure of  $\Phi(x)$  near the wall affects emitted electrons near the wall. 1 V is sufficient to pull back a substantial fraction of cold secondaries emitted with an energy distribution corresponding to  $T_{\text{emit}} = 2 \text{ eV}$ .

The plasma potential relative to the right wall in simulation B is on average *negative*. The inverse sheaths at the walls are the only stable long-term structures in  $\Phi(x)$ ; in the plasma interior, the fluctuating electric field from plasma instabilities or waves averages to zero. Thus, we find that  $\Phi(x = H/2)$ , averaged over long intervals of  $2 \mu\text{s}$ , is  $-1 \text{ V}$ , equal to the inverse sheath amplitude  $\Phi_{-1}$ . In general, because electron velocities usually far exceed ion velocities in plasmas, maintaining zero current with negative plasma potential is rare in applications. It is possible, for instance, if the escape rate of plasma electrons is suppressed below that of ions by a nonuniform magnetic field [22] or if electrons are still confined within a potential well that is below the wall potential [23]. However, neither is the case in simulation B.

To see how the zero current condition is maintained in the inverse sheath regime, consider the time evolution of the fluxes in Fig. 2. In simulation B, there are three

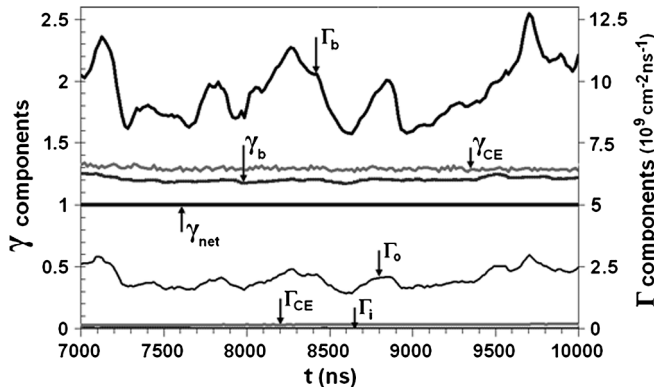


FIG. 2. Temporal evolution of the particle fluxes and partial SEE coefficients at the left wall in simulation B.

components of  $\Gamma_{\text{in}}$ : CEEs ( $\Gamma_{\text{CE}}$ ), secondaries from the *opposite* wall ( $\Gamma_b$ ), and “other” electrons ( $\Gamma_o$ ).  $\Gamma_o$  consists of secondaries pulled back to the wall by the inverse sheath. These electrons are cold and induce no SEE ( $\gamma_o = 0$ ). This is why  $\gamma_{\text{net}}$  does not exceed unity even though  $\gamma_b, \gamma_{\text{CE}} > 1$  in Fig. 2. In fact,  $\gamma_{\text{net}}$  appears to be exactly unity. To see why, first consider the ion flux. In simulation A, ions are accelerated in the sheath to the wall, forming a substantial flux  $\Gamma_i$ . The sheath limits  $\Gamma_{\text{CE}}$  to maintain (2) approximately; see Table I. In simulation B, because there are no sheaths, ions are not drawn to the wall and the Bohm criterion does not apply.  $\Gamma_i$  is merely 3% of  $\Gamma_{\text{CE}}$ . ( $\Gamma_i$  is nonzero because with  $T_{\text{ion}}$  set to 1 eV in the simulation some ions have sufficient *thermal* energy to overcome the barrier  $\Phi_{-1}$  and reach the wall.) With very small  $\Gamma_i$ , the net electron flux  $\Gamma_e$  must be near zero in simulation B if the current (1) is to be balanced. Hence  $\gamma_{\text{net}} = 0.9994 \approx 1$  at  $t = 10 \mu\text{s}$ .

Note that zero net electron flux is maintained by the inverse sheath in a *stable* manner at all times, not just on average. In Fig. 2,  $\gamma_{\text{net}} = 1$  and never varies, even though the main electron *influx* component  $\Gamma_b$  rapidly fluctuates due to the interior plasma fluctuations. Notice that the fluctuations of  $\Gamma_o$  closely follow fluctuations of  $\Gamma_b$ . It turns out the following relation is maintained,

$$\Gamma_b(1 - \gamma_b) + \Gamma_o \approx 0. \quad (5)$$

That is, the number of pulled-back secondaries always self-adjusts to make  $\gamma_{\text{net}} = 1$ . Since  $\gamma_b \approx 1.2$  roughly in Fig. 2,  $\Gamma_o(t) \approx 0.2\Gamma_b(t)$ . Equation (5) is just the equilibrium current equation (1) with  $\Gamma_{\text{in}} = \Gamma_b + \Gamma_o$ ,  $\Gamma_{\text{out}} = \gamma_b\Gamma_b$ , and the much smaller terms  $\Gamma_i, \Gamma_{\text{CE}}(1 - \gamma_{\text{CE}})$  neglected.

The reason for stability is qualitatively simple. If a perturbation in  $\Gamma_b$  or  $\gamma_b$  causes the floating wall’s charge to increase (become more positive), then  $\Phi_{-1}$  increases in magnitude. A larger fraction of the emitted secondaries is pulled back to the wall, causing the wall charge to decrease, canceling the perturbation. Hence the inverse sheaths are stable in a current-voltage sense. This is in contrast to classical sheaths in the system which were found to become unstable, leading to oscillations of the sheath potential and net current [16,17].

The disappearance of the Debye sheath has important implications. Sheaths “insulate” the walls from a plasma by reflecting most incoming electrons. Figure 3 shows the EV<sub>x</sub>DF (the EVDF integrated over  $V_y$  and  $V_z$ ) in both simulations. In general, in low collisionality, the EVDF is nonlocal [24]. In simulation A with classical sheaths, bulk plasma electrons in the interior of the plasma volume with  $\frac{1}{2}m_e V_x^2 < e\Phi$  are trapped and oscillate in the potential well. They cannot hit the wall unless they have large  $V_{\parallel}$  and get scattered into the loss cone ( $W_x > e\Phi$ ) by a neutral collision. Because collisionality is low, replenishment of the loss cone is weak and there is a sharp cutoff in the Gaussian bulk EV<sub>x</sub>DF at  $V_x = \pm V_{\text{cutoff}} \equiv (2e\Phi/m_e)^{1/2}$ .

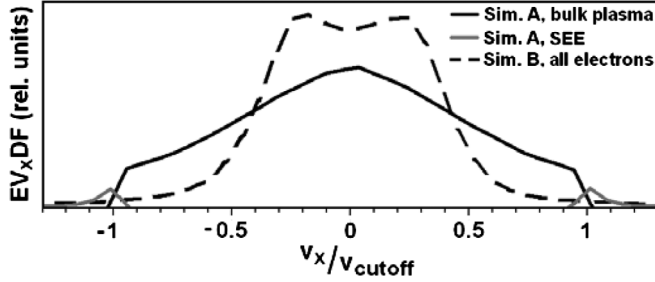


FIG. 3.  $EV_x DF$  for electrons in the “middle” of the system ( $0.8 < x < 1.7$  cm) at  $t = 10 \mu\text{s}$  in both runs.  $V_x$  is in units of  $V_{\text{cutoff}} \approx 2.7 \times 10^8$  cm/s (the cutoff velocity for simulation A with  $\Phi \approx 21$  V). For simulation A, secondaries and bulk plasma electrons are plotted separately. In simulation B, all electrons are secondaries. The “valley” in the  $EV_x DF$  is responsible for the strong two-stream fluctuations [21].

Secondaries form small humps beyond the cutoff velocity. Overall, the walls are protected from most electrons in the system. Bulk electrons gain energy  $W_{\parallel}$  parallel to the walls by drift rotation and turbulent collisions. The bulk equilibrium temperature depends on a balance between the collisional heating and collisional losses;  $T_{\parallel}$  scales as  $E_z^2 \nu_{\text{turb}} / \nu_{\text{en}}$  [15]. So one would expect the plasma in simulation B to be  $\sim 3$  times as hot as in simulation A.

However, because the sheaths vanish in simulation B, every aspect of the plasma is different. Electrons travel freely to the walls, so all electrons are secondaries recently emitted from a wall. The  $EV_x DF$  takes the form of two opposing SEE beams, similar in shape to the SEE beams in simulation A. There is no cutoff velocity. Because  $V_x$  comes only from the small velocity of emission, the average kinetic  $x$  energy  $\langle W_x \rangle$  is less for simulation B than simulation A in Fig. 3. Also, because no electrons are trapped, most will reach the other wall before suffering any collisions that increase  $W_{\parallel}$ . Therefore,  $\langle W_{\parallel} \rangle$  is also much smaller. EDIPIC diagnostics record the average kinetic energy of all electrons in the plasma. At  $t = 10 \mu\text{s}$  in both simulations, the losses and heating are in balance. Simulation A has  $\langle W_x \rangle = 5$  eV and  $\langle W_{\parallel} \rangle = 89$  eV. Simulation B has  $\langle W_x \rangle = 2.5$  eV and  $\langle W_{\parallel} \rangle = 46$  eV. The most important feature of simulation B is that the particle and energy fluxes to the walls are enormous. With no sheaths and  $\gamma_{\text{net}} = 1$ , all electrons in the system can be thought of as traveling back and forth from wall to wall repeatedly. So  $\Gamma_{\text{in}}$  is 17 times larger in simulation B compared to simulation A; see Table I. The secondaries, though emitted cold, will gain drift energy and displace along  $E_z$  before impacting the other wall. Thus the energy flux is found to be 20 times larger in simulation B and the axial transport  $\sim \langle V_z \rangle$  is 8 times larger.

We have found with  $B_x$  fixed at 100 G, the inverse sheath tends to appear in simulations with electric field  $E_z$  exceeding 200 V/cm. The transition occurs because even the “coldest” electrons in the system have drift energies

parallel to the wall oscillating from 0 to  $2m_e V_D^2$ . Therefore, when  $V_D$  reaches a critical value, the average emission induced by secondary electron beams  $\gamma_b$  will exceed unity. When this happens, a classical sheath, see Eq. (4), cannot maintain zero current. This result may have a connection to an important effect attributed to SEE in HT experiments. For wall materials with substantial SEE yield such as BNC, SEE becomes degrading at high voltages, leading to saturation of the temperature  $T_e$  and maximum electric field [25]. In experiments, the discharge voltage is fixed.  $E_z$  and  $T_e$  are axially nonuniform, determined self-consistently with the axial transport and the balance between heating and losses. In EDIPIC, the fields are fixed and uniform, but the simulations suggest that as the voltage is increased in a HT, the  $\mathbf{E} \times \mathbf{B}$  drift energy of electrons will reach a critical value in which the insulating sheaths begin to collapse. Further increases in  $E_z$  and  $T_e$  would be suppressed by the enhanced transport and energy loss.

The implications of these simulations are not limited to  $\mathbf{E} \times \mathbf{B}$  discharges. The  $\mathbf{E} \times \mathbf{B}$  field just maintained the plasma temperature in the inverse sheath simulation. In general, at high temperatures, energetic electrons can eject multiple secondaries from many materials including insulators [5,20] and metals [5,8,26]. Conventional sheath theories may break down if the incident electrons produce more than one secondary on average. In this situation, the intrinsic properties of a Debye sheath (which are also present in the “space-charge-limited” sheaths usually assumed to form under strong SEE [3,4,7–9]) are no longer needed to maintain zero current. It is not necessary for ions to be drawn to the wall, for a presheath to exist, for plasma electrons to be confined, or for the wall potential to be below the plasma potential. Instead, zero current can be maintained in a fundamentally different way by an “inverse sheath,” a positive surface charge shielded from the plasma by negative space charge at the interface. The wall potential is above the plasma potential, so the ion flux is negligible and secondaries are pulled back to the wall to maintain zero net electron flux. Most importantly, plasma electrons travel unobstructed to the walls, causing extreme losses. Losses are critical to the performance of plasma devices.

The authors are indebted to Dmytro Sydorenko, the developer of the EDIPIC code. This work was supported by the U.S. Department of Energy.

- 
- [1] K. U. Riemann, *J. Phys. D* **24**, 493 (1991).
  - [2] V. A. Rozhansky and L. D. Tsensin, *Transport Phenomena in Partially Ionized Plasma* (Taylor & Francis, London, 2001).
  - [3] M. A. Lieberman and A. J. Lichtenberg, *Principles of Plasma Discharges and Material Processing* (Wiley, Hoboken, NJ, 2005).
  - [4] P. C. Stangeby, *The Plasma Boundary of Magnetic Fusion Devices*, Plasma Physics Series (IOP, Bristol, 2000).

- [5] J. R. M. Vaughan, *IEEE Trans. Electron Devices* **36**, 1963 (1989).
- [6] R. H. Cohen and D. D. Ryutov, *Contrib. Plasma Phys.* **44**, 111 (2004).
- [7] G. D. Hobbs and J. A. Wesson, *Plasma Phys.* **9**, 85 (1967).
- [8] P. J. Harbour and M. F. A. Harrison, *J. Nucl. Mater.* **76**, 513 (1978).
- [9] E. Ahedo, *Phys. Plasmas* **9**, 4340 (2002).
- [10] N. Hershkowitz and M. H. Cho, *J. Vac. Sci. Technol. A* **6**, 2054 (1988).
- [11] L. A. Schwager, *Phys. Fluids B* **5**, 631 (1993).
- [12] A. I. Morozov and V. V. Savel'ev, *Fiz. Plazmy* **33**, 24 (2007).
- [13] D. Sydorenko, A. Smolyakov, I. Kaganovich, and Y. Raitses, *Phys. Plasmas* **13**, 014501 (2006).
- [14] D. Sydorenko, A. Smolyakov, I. Kaganovich, and Y. Raitses, *IEEE Trans. Plasma Sci.* **34**, 815 (2006).
- [15] I. D. Kaganovich, Y. Raitses, D. Sydorenko, and A. Smolyakov, *Phys. Plasmas* **14**, 057104 (2007).
- [16] M. D. Campanell, A. V. Khrabrov, and I. D. Kaganovich, *Phys. Rev. Lett.* **108**, 235001 (2012).
- [17] D. Sydorenko, Ph.D. thesis, University of Saskatchewan, 2006.
- [18] J. P. Boeuf and L. Garrigues, *J. Appl. Phys.* **84**, 3541 (1998).
- [19] A. Smirnov, Y. Raitses, and N. Fisch, *Phys. Plasmas* **11**, 4922 (2004).
- [20] A. Dunaevsky, Y. Raitses, and N. J. Fisch, *Phys. Plasmas* **10**, 2574 (2003).
- [21] D. Sydorenko, A. Smolyakov, I. Kaganovich, and Y. Raitses, *Phys. Plasmas* **14**, 013508 (2007).
- [22] S. H. Seo, J. H. In, and H. Y. Chang, *J. Appl. Phys.* **97**, 023305 (2005).
- [23] L. Oksuz and N. Hershkowitz, *Phys. Lett. A* **375**, 2162 (2011).
- [24] V. I. Demidov, C. A. DeJoseph, Jr, and A. A. Kudryavtsev, *Phys. Rev. Lett.* **95**, 215002 (2005).
- [25] Y. Raitses, I. D. Kaganovich, A. Khrabrov, D. Sydorenko, N. J. Fisch, and A. Smolyakov, *IEEE Trans. Plasma Sci.* **39**, 995 (2011).
- [26] M. A. Furman and M. T. F. Pivi, Technical Report No. SLAC-PUB-9912; LBNL-52807, 2003.